Basic magnetization curve fitting function based on spectral analysis

Gang Xu[1), 2)] (ORCID ID:0000-0003-0350-248X), **Shiwei Wang**[1), 2), *)] (0009-0001-9802-2202), **Long Zhang**[1), 2)], **Long Wu**[1), 2)] (0009-0002-9680-1154)

DOI: https://doi.org/10.14314/polimery.2025.2.3

Abstract: The current fitting function of the basic magnetization curve does not provide the exact fit necessary for the simulation modeling of electromechanical devices containing conductive materials, including polymers. Therefore, an odd polynomial fitting function based on the spectral analysis of the fitting results of the basic magnetization curve under sinusoidal excitation is proposed, and the effect of the odd polynomial fitting is studied by comparative analysis. The results show that the odd polynomial provides a better fit and has a simple expression, and the method of obtaining the fitting function based on the spectral analysis provides a new idea for the selection of the basic magnetization curve fitting function.

Keywords: basic magnetization curve, fit function, spectral analysis, odd polynomial, conductive polymers.

Podstawowa funkcja dopasowania krzywej namagnesowania oparta na analizie widmowej

Streszczenie: Obecna funkcja dopasowania podstawowej krzywej namagnesowania nie zapewnia dokładnego dopasowania niezbędnego do modelowania symulacyjnego urządzeń elektromechanicznych zawierających materiały przewodzące, w tym polimery. Dlatego zaproponowano funkcję dopasowania wielomianu nieparzystego opartą na analizie widmowej wyników dopasowania podstawowej krzywej namagnesowania przy wzbudzeniu sinusoidalnym, a wpływ dopasowania wielomianu nieparzystego zbadano za pomocą analizy porównawczej. Wyniki pokazują, że wielomian nieparzysty zapewnia lepsze dopasowanie i ma proste wyrażenie, a metoda uzyskiwania funkcji dopasowania oparta na analizie widmowej dostarcza nowego pomysłu na wybór funkcji dopasowania podstawowej krzywej namagnesowania.

Słowa kluczowe: podstawowa krzywa namagnesowania, funkcja dopasowania, analiza widmowa, wielomian nieparzysty, polimery przewodzące.

Soft magnetic materials are widely used in machines, electrical devices, and electrical automation devices due to their low coercivity and high permeability [1–5]. As the variable inductance of the flux-memory machine and the change characteristics of the magnetic chain, the excitation characteristics of the transformer and the output characteristics of the magnetoresistance (MR) sensor and other electromechanical equipment containing soft magnetic materials, the response characteristics of soft magnetic materials similar to the magnetization characteristics [6–8] are presented, usually described by the basic magnetization curve [9–13].

The basic magnetization curve, commonly referred to as the fundamental magnetization curve, is an important feature of soft magnetic materials that defines the relationship between magnetic field advantage and magnetic flux density during the magnetization procedure. This curve shows important nonlinear behavior, indicating the material's response to changing external magnetic fields. It is critical for precisely simulating the activity of soft magnetic materials in electromechanical devices like transformers, inductors, and magnetoresistance (MR) sensors. The curve is critical for comprehending a material's magnetic properties because it offers information about saturation, hysteresis, and permeability, all of which are required to design effective and accurate simulation models for these devices.

The basic magnetization curve has prominent nonlinear characteristics, and the simulation modeling containing soft magnetic materials must accurately describe the basic magnetization curve. The expression is simple, and

[1)] School of Mechanical and Electrical Engineering, Huainan Normal University, Huainan 232038, Anhui, China.

[2)] Human-Computer Collaborative Robot Joint Laboratory of Anhui Province, Huainan Normal University, Huainan 232038, Anhui, China.

[*)] Author for correspondence: destiny-summer@hnnu.edu.cn

the good fitting effect of the fitting function is to ensure the feasibility of the simulation model and the key to accuracy [14].

The polynomial fitting function is widely used for various types of curve fitting due to their generalizability [15–19]. The fitting of polynomials can be further improved by increasing the order of the fit. Still, an order that is too high increases the number of solution parameters and exacerbates the ill-posedness of the fitting operation [20]. Based on the geometrical similarity between the fitted function curves and the basic magnetization curves, hyperbolic tangent type fitting functions and arctangent type fitting functions are applied to fit the basic magnetization curves. Sandeep *et al.* compared the fitting effects of different fitting functions applied to the nonlinear output characteristics of the magnetization of a self-excited induction generator, and the results showed that a hyperbolic tangent type fitting function is the best fit [21]. Zhao *et al.* improved the fitting of the basic magnetization curve of the permalloy by adding linear and adjustment terms to the hyperbolic tangent type and arctangent type fitting functions but, at the same time, increased the complexity of the expressions [22]. In addition to the common fitting functions mentioned above, the fitting functions used for fundamental basic magnetization curve fitting include the hyperbolic sine fitting function [7] and logarithmic polynomial fitting function [23], among others. Tang *et al.* compared and analyzed the fitting effects of 11 basic magnetization curve fitting functions and found that the best fitting functions are not the same for different permeabilities and magnetization regions [24].

The Langevin function, $L(x) = \coth(x) - (1/x)$, is widely utilized to simulate the nonlinear magnetization of soft magnetic materials. Silveyra and colleagues showed their accuracy in describing the anhysteretic magnetization curves of varied materials, both isotropic and anisotropic, by integrating an internal field that interacts with the external magnetic field [25, 26].

Their research presented a physically based model depending on this function, which was executed in the MagAnalyst toolbox to enable effective curve fitting of magnetization data [27]. This approach offers a more accurate alternative to polynomial functions in magnetization evaluation.

Conductive polymers are usually characterized by magnetization curves which help to understand the spin phenomena occurring in them. Éfendiyev *et al*. [28] compared experimental and computational curves when studying magnetic nanoparticles – polymer magnetic microspheres (PMMS) with magnetite nanoparticles prepared using collagen and polystyrene. Filipcsei *et al*. [29] conducted an extensive study of magnetically responsive polymer composites, dividing them into ferrofluids, magnetorheological fluids, magnetic gels, and magnetic elastomers. In Prasanna *et al*. work [30], polyaniline/$CoFe_2O_4$ nanocompounds were obtained, demonstrating improvement of the magnetic properties of the composite, especially in terms of saturation magnetization and coercivity.

In summary, the existing basic magnetization curve fitting functions make it challenging to balance simple expressions and accurate fitting results, while the selection of the fitting function expressions needs to be based on a lack of comparison and adjustment through tedious.

Aiming at the above problems, this paper analyzes the spectrum of the output of the basic magnetization curve fitting results under sinusoidal excitation. Based on the analysis of the spectral characteristics, a new fitting function is proposed and analyzed to verify its validity and reasonableness. The fitting effect and function characteristics are studied by comparing them with diverse types of fitting functions. Finally, it is applied to the MR sensor to verify the fitting effect further.

EXPERIMENTAL PART

Method for obtaining fitting function based on spectral analysis

Magnetization process

The magnetization process describes how a material responds to a magnetic field by changing its internal magnetic structure. When an external magnetic field is applied, the atomic-scale magnetic moments within the material align in the field's direction, resulting in the formation of a net magnetization. In ferromagnetic materials, this alignment is caused by exchange interactions between neighboring atoms, which results in spontaneous magnetization even in the lack of an external field. Magnetization behavior differs with material composition, crystalline structure, and temperature. The basic magnetization curve depicts the relationship between magnetization and the applied field, including important characteristics like initial magnetization, saturation, and hysteresis impacts.

As the applied field rises, the material goes through several stages of magnetization. In the low-field region, domain wall motion takes precedence, in which preexisting magnetic domains grow or shrink in response to the field. This stage is distinguished by reversible magnetization shifts, followed by an intermediate region in which domain rotation becomes important, resulting in a rise in magnetization. Beyond a crucial threshold, referred to as the saturation point, all magnetic moments align with the field to achieve maximum magnetization. At this point, increasing the external field has negligible effect on magnetization. The basic magnetization curve mathematically represents these transitions, making it easier to model and analyze magnetic materials for a variety of applications.

Comprehending the magnetization procedure is essential for improving the performance of magnetic materials

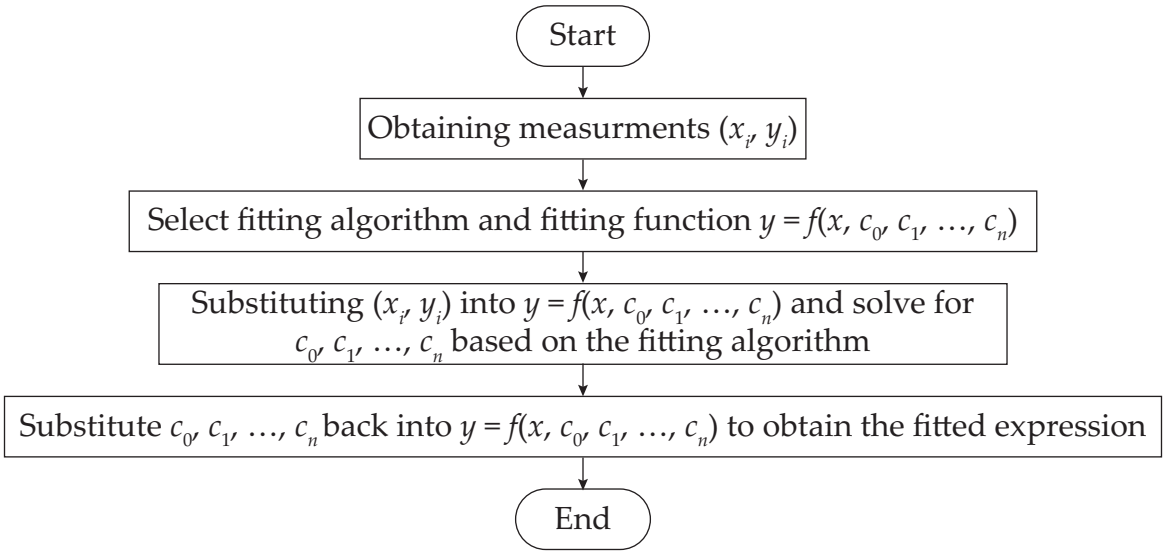

Fig. 1. Basic magnetization curve fitting flow chart

in electromechanical devices, sensors, and transformers. The selection of an appropriate fitting function for the basic magnetization curve allows precise simulation and prediction of magnetic behavior under various operating conditions. Using spectral analysis methods, an efficient and computationally effective fitting function can be developed to precisely represent the magnetization curve. This method not only improves the mathematical modeling of magnetization procedures but also makes it easier to create sophisticated materials and devices that require accurate magnetic properties.

Basic magnetization curve fitting process

The process of fitting the basic magnetization curve is shown in Fig. 1. First, the magnetization measurement data of the magnetic material or the input/output measurement data of the MR sensor (x_i, y_i) are acquired, where i = 1, 2, …, m is the measurement data' serial number; The appropriate basic magnetization curve fitting algorithm and fitting function $y = f(x, c_0, c_1, c_2, \ldots, c_n)$ are then determined, where c_0, c_1, c_2, …, c_n are the n coefficients of the fitting function; Then the measurement data (x_i, y_i) is substituted into the fitting function $y = f(x, c_0, c_1, c_2, \ldots, c_n)$ and the coefficients c_0, c_1, c_2, …, c_n is solved using the fitting algorithm; Finally, the obtained coefficients c_0, c_1, c_2, …, c_n is substituted back into the fitting function $y = f(x, c_0, c_1, c_2, \ldots, c_n)$ to get the fitted expression for the basic magnetization curve.

Typical basic magnetization curve fitting functions include polynomial fitting functions, hyperbolic tangent type fitting functions, and arctangent type fitting functions [21, 24].

The general formula for the polynomial fitting function is presented in Equation 1:

$$y = p_0 + p_1 x + p_2 x^2 + L + p_n x^n = p_0 + \sum_{i=1}^{n} p_i x^i \quad (1)$$

where p_0, p_1, p_2, …, p_n are the coefficients of the polynomial fitting function.

Hyperbolic tangent type fitting functions and arctangent type fitting functions again include the basic form and deformed forms. The basic form of a hyperbolic tangent type fitting function is presented in Equation 2:

$$y = h_0 \tanh(h_1 x) \quad (2)$$

Where h_0, and h_1 are the coefficients of the hyperbolic tangent type fitting function.

The basic form of an arctangent type fitting function is depicted in Equation 3:

$$y = a_0 \arctan(a_1 x) \quad (3)$$

where a_0 and a_1 are the coefficients of the arctangent type fitting function.

The basic magnetization curve has prominent nonlinear characteristics, and the selection of the widely used nonlinear least squares (NLS) method as the fitting algorithm can ensure the fitting results' accuracy while reducing the fitting process's complexity [34]. The basic principle of NLS is to determine the optimal parameters of the model by minimizing the sum of squares of the residuals between the observed data and the predicted values of the nonlinear model. Implementing the NLS method begins with determining the form of the nonlinear model used for fitting. Then, for a given set of observations, the difference between the model predictions and the actual observations is calculated for each data point; this difference is called the residual. Next, the optimal parameters of the model are determined by minimizing the sum of squares of the residuals. Since nonlinear models usually have complex parameter spaces, it is not possible to solve the least squares problem directly by analytical methods. Therefore, the gradient descent method is used to search for the optimal parameters. Finally, the quality of the fit-

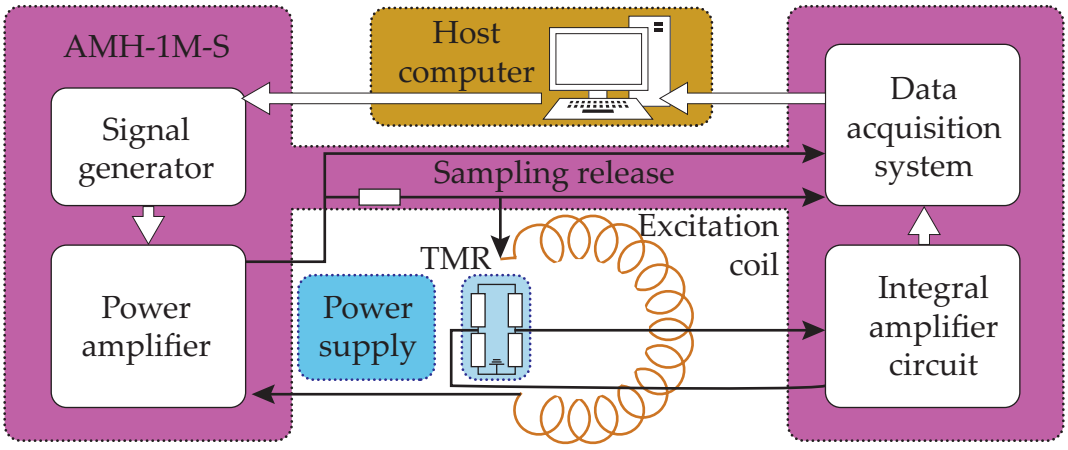

Fig. 2. Schematic diagram of TMR input/output data measurement device

ting results is assessed, and the accuracy and reliability of the fit are comprehensively evaluated by residual analysis, comparison of the fitted curves with the observed data, and confidence intervals for the parameters.

In this study, standard magnetization measurement methods were used to collect experimental data for curve fitting. The magnetization measurements of the soft magnetic material or MR sensor input/output were carried out under controlled laboratory conditions, with differing magnetic field strengths applied and the corresponding magnetic responses measured. These data were then utilized to fit the basic magnetization curve with nonlinear least squares (NLS) and other fitting functions.

TMR input/output data acquisition

The tunneling magnetoresistive sensor (TMR) TMR2905 input/output data are measured using the device shown in Fig. 2, which consists of five parts: the host computer, the AMH-1M-S magnetic characteristic test system, the power supply, the TMR, and the excitation coil. The internal AMH-1M-S includes five parts: signal generator, power amplifier, sampling resistor, integration amplification circuit, and data acquisition system. The host computer controls the signal generator in AMH-1M-S to produce an excitation signal with adjustable amplitude, which is processed by the power amplifier and then transmitted to the excitation coil through the sampling resistor, which collects the excitation current i of the excitation coil and sends it to the data acquisition system. The excitation coil is an N-turn screw-wound ring with an average radius of r and an opening, and a TMR is placed at the opening position of the screw-wound ring. The direction of the TMR sensitivity axis is aligned with the direction of the excitation magnetic field in the excitation coil. The power supply provides 5 V DC power for the TMR, and the differential output voltage U of the TMR is processed by an integrating amplifier circuit and transmitted to the data acquisition system. The data acquisition system collects the excitation signal from the excitation coil and the TMR measurement signal and uploads them to the host computer for further processing. The length of the closed magnetic circuit inside the excitation coil is $2\pi r$, and the TMR input magnetic field strength $H = Ni/2\pi r$ can be obtained according to the Ampere loop theorem.

RESULTS AND DISCUSSION

Spectral analysis of the basic magnetization curve

Define the numbering of the 4th order polynomial fitting function and the basic forms of the hyperbolic tangent type fitting functions and the arctangent type fitting functions as P1, H1, and A1, respectively. P1, H1, and A1 are selected as the fitting functions for the fundamental magnetization curve utilizing the NLS technique, utilizing DC magnetization data of DT4 pure iron, a soft magnetic material with low coercivity and high permeability [35]. The results of the fitted expressions based on the P1, H1, and A1 are shown in Table 1. The curve fitting results of the fitted expressions based on the P1, H1, and A1 are shown in Fig. 3. Fig. 3 shows that the 4th order polynomial fitting function P1 is the worst fit due to its low order, and the fitting effect of the arctangent type fitting function basic form A1 is slightly better

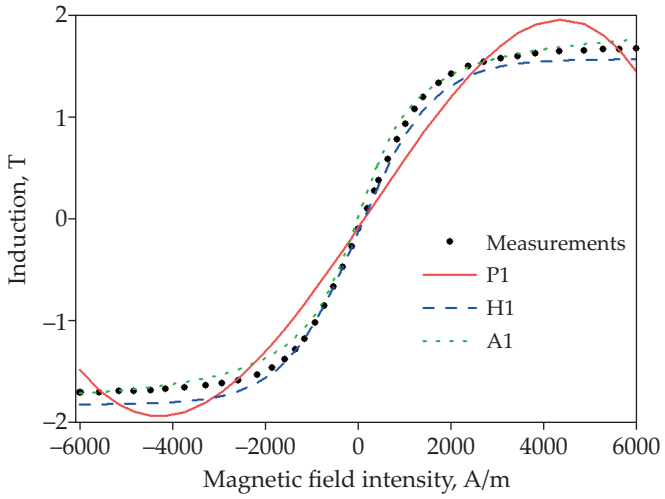

Fig. 3. Curve fitting outcomes for P1, H1, and A1

T a b l e 1. Fitting expression results based on P1, H1, and A1

Number	Fitting expression results
P1	$y = -0.114 + 2.276x + 0.119x^2 - 0.462x^3 - 0.02521x^4$
H1	$y = -1.696 \tanh(-6.235 \cdot 10^{-4}x)$
A1	$y = 1.225 \arctan(0.001073x)$

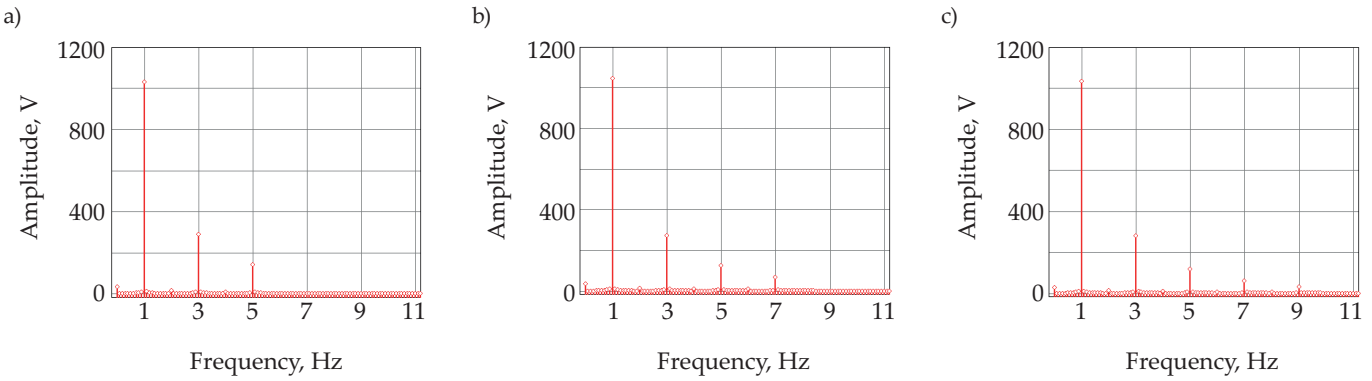

Fig. 4. Spectral analysis of the P1 (a), H1 (b) and A1 (c) outputs with sinusoidal excitation

than that of the hyperbolic tangent type fitting function basic form H1. Although there are significant differences in the curve fitting results of the P1, H1, and A1 three fitting functions, they all reflect the trend of the DT4 magnetization measurement data and the nonlinear characteristics of the basic magnetization curves.

Further comparison of the differences in the transmission properties of P1, H1, and A1 results. A sinusoidal excitation signal $x = A_m \sin(2\pi ft)$ with amplitude A_m and frequency f is applied to the three fitted expressions in Table 1, and the outputs of the P1, H1, and A1 three fitted expressions are analyzed spectrally.

Fig. 4 shows the spectral analysis results of the output of the fitted expressions of P1, H1, and A1 for sinusoidal excitation. The P1 output spectrum is significant in fundamental, 3rd harmonic, and 5th harmonic amplitudes; the H1 output spectrum is significant in fundamental, 3rd harmonic, 5th harmonic, and 7th harmonic amplitudes; and the A1 output spectrum is significant in fundamental, 3rd harmonic, 5th harmonic, 7th harmonic and 9th harmonic amplitudes. The fitted expressions and the output spectral results for P1, H1, and A1 are all different but reflect the common feature of significant fundamental and odd harmonic amplitudes. If the basic magnetization curve of DT4 is equated to a polynomial fitting function of infinite order, based on the distinctive characteristics of the fundamental and odd harmonic amplitudes, consider that the odd terms of this polynomial come into effect. Therefore, the even terms in the polynomial fitting function are eliminated from the polynomial fitting function, and the odd polynomial fitting function is proposed (Eq. 4).

$$y = o_0 + o_1 x + o_2 x^3 + L + o_n x^{2n-1} = o_0 + \sum_{i=1}^{n} o_i x^{2i-1} \quad (4)$$

where o_0, o_1, o_2, …, o_n is the coefficient of the odd polynomial.

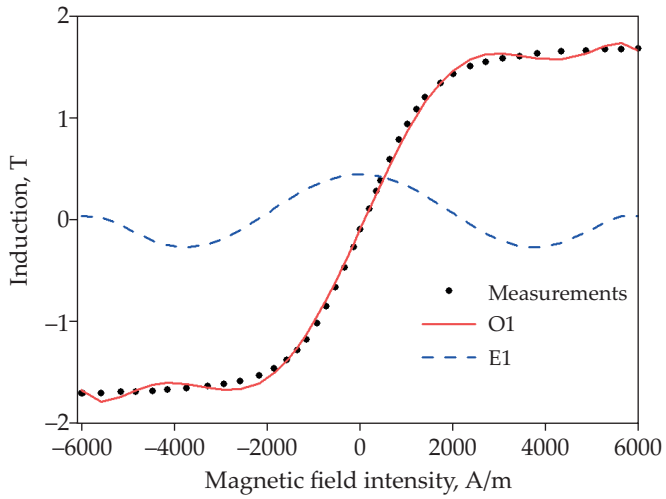

Fig. 5. Curve fitting outcomes for O1 and E1

Odd polynomial functions

To verify the validity of the odd polynomial fitting function applied to the basic magnetization curve fitting, as well as the rationality of eliminating the even terms in the polynomial fitting function, a 5th-order odd polynomial O1 and a 6th-order even polynomial E1 are chosen as the fitting functions to fit the basic magnetization curves based on the NLS method to the DC magnetization measurement data of DT4. O1 and E1 are respectively (Eq. 5 and 6):

$$y = o_0 + o_1 x + o_2 x^3 + o_3 x^5 \quad (5)$$

$$y = e_0 + e_1 x^2 + e_2 x^4 + e_3 x^6 \quad (6)$$

where e_0, e_1, e_2, e_3 is the coefficient of the 6th order even polynomial fitting function.

The results of curve fitting based on both O1 and E1 are shown in Fig. 5. O1 fits significantly better than E1, and O1 better reflects the trend of the DT4 magnetization measurement data and the nonlinear characteristics of the basic magnetization curve. The validity of the odd polynomial applied to the basic magnetization curve is illustrated, as well as the justification for the elimination of the even terms in the polynomial fitting function.

Compared to O1, the E1 fit is extremely poor and does not reflect the trend of the DT4 pure iron magnetization measurement data as well as the nonlinear characteristics of the underlying basic magnetization curve. Combining the Equation 5 and 6 as well as Fig. 4, it is easy to see that, without considering the constant term o_0, the odd and even polynomial fitting functions are odd and even functions, respectively. The curve fitting results corresponding to the odd polynomial fitting function exhibit centrosymmetric features, while the curve fitting results corresponding to the even polynomial fitting function exhibit axisymmetric features. The basic magnetization curve exhibits a centrosymmetric character, and its expression can also be approximated as an odd function. Thus, the similarity in functional properties between the odd polynomial and the expression of the basic magnetization curve justifies the application of the odd polynomial to the fitting of the basic magnetization curve.

Comparative analysis of odd polynomial

Comparison of fitting effects of odd polynomial

To more comprehensively analyze the fitting effect of odd polynomial, polynomial fitting functions of different orders and odd polynomial fitting functions, as well as a variety of hyperbolic tangent type fitting functions and arctangent type fitting functions, are chosen to fit the DC magnetization data of DT4 pure iron based on the NLS method. The types and numbers of the selected fitting functions are shown in Table 2, and the curve fitting results are shown in Fig. 5.

The degree of fit of the curve fitting results to the magnetization measurement data is quantitatively evaluated using the coefficient of determination R^2 [36], expressed in Equation 7:

$$R^2 = 1 - \sum_{i=1}^{n} \frac{(y_i - \hat{y}_i)^2}{(y_i - \bar{y}_i)^2} \tag{7}$$

where y_i are the magnetization measurement data; $\hat{y}_i$ are the curve fitting results; $\bar{y}_i = \sum_{i=1}^{n} \frac{y_i}{n}$ is the average value of the magnetization measurement data; and n and i are the total number of data points and the serial number, respectively. The value of R^2 ranges from 0 to 1. When R^2 equals 1 or close to 1, the curve fitting result has the highest reliability and the best fitting effect.

Defining $x \in [-6000, 6000]$ as the overall interval; $x \in [-2000, 2000]$ as the linear interval; and $x \in [-6000, 6000] \cup [-2000, 2000]$ as the nonlinear interval, the R^2 of the chosen fitting function for the different intervals is shown in Table 2. The mean values of R^2 for the 15 fitted functions are 0.943, 0.96, and 0.91 for the overall, linear, and nonlinear intervals, respectively, and the results that are greater than the respective mean values of R^2 for each interval are shown in boldface type, while those that have the maximum value of the respective R^2 for each interval are shown in italics. It can be seen through Table 2 that $R^2 = 0.992$ is the largest for O3 among

T a b l e 2. Comparison of fitting functions

Type	Designation	Expression	Number of coefficients	R^2		
				Overall interval	Linear interval	Nonlinear interval
Polynomial	P1	$y = p_0 + p_1x + p_2x^2 + \mathrm{L} + p_4x^4$	5	0.827	0.864	0.752
	P2	$y = p_0 + p_1x + p_2x^2 + \mathrm{L} + p_5x^5$	6	0.925	0.955	0.878
	P3	$y = p_0 + p_1x + p_2x^2 + \mathrm{L} + p_6x^6$	7	0.955	0.989	0.905
	P4	$y = p_0 + p_1x + p_2x^2 + \mathrm{L} + p_7x^7$	8	0.984	0.995	0.944
	P5	$y = p_0 + p_1x + p_2x^2 + \mathrm{L} + p_8x^8$	9	0.987	0.996	0.95
	P6	$y = p_0 + p_1x + p_2x^2 + \mathrm{L} + p_9x^9$	10	0.992	0.996	0.966
Hyperbolic tangent type	H1	$y = h_0 \tanh(h_1x)$	2	0.901	0.944	0.896
	H2	$y = h_0 \tanh(h_1x + h_2) + h_3x + h_4$ [32]	5	0.951	0.993	0.892
	H3	$y = h_0 \tanh(h_1x) + h_2 \tanh(h_3x) + h_4x$ [22]	5	0.967	0.905	0.995
Arctangent type	A1	$y = a_0 \arctan(a_1x)$	2	0.921	0.951	0.91
	A2	$y = a_0 \arctan(a_1x) + a_2 \arctan(a_3x) + a_4x$ [22]	5	0.857	0.867	0.832
	A3	$y = a_0 \arctan(a_1x) + a_2x$ [33]	3	0.958	0.985	0.893
Odd polynomial	O1	$y = o_0 + o_1x + o_2x^3 + o_3x^5$	4	0.951	0.975	0.915
	O2	$y = o_0 + o_1x + o_2x^3 + \mathrm{L} + o_4x^7$	5	0.985	0.995	0.954
	O3	$y = o_0 + o_1x + o_2x^3 + \mathrm{L} + o_5x^9$	6	0.992	0.997	0.964

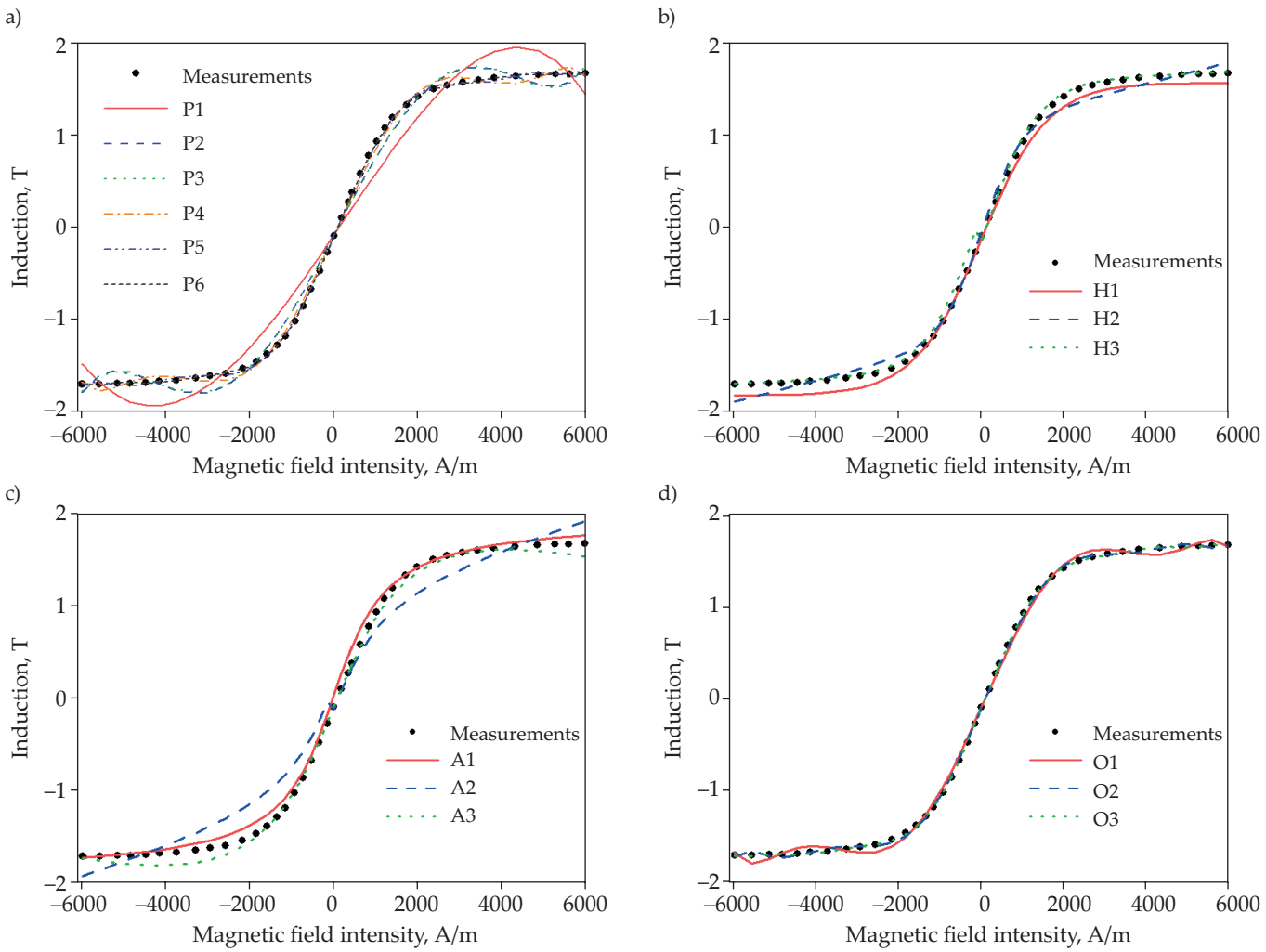

Fig. 6. Curve fitting results: a) polynomial functions P1~P6, b) hyperbolic tangent type functions H1~H3, P1~P6, H1~H3, c) arctangent type functions A1~A3, d) odd polynomial functions O1~O3

the odd polynomials in the overall interval; Within the linear interval, again the $R^2 = 0.997$ for O3 is the largest; The range of nonlinear interval is then the largest for the $R^2 = 0.997$ for H3 in the hyperbolic tangent type. One and only one of the diverse types of fitted functions has R^2 above the meaning for all the fitted functions in the odd polynomial over a range of various intervals.

Fig. 6 shows that the polynomial P1 and P2 fit significantly worse; the hyperbolic tangent type fitting function H1 is considerably worse; the arctangent type fitting function A1 and A2 are significantly worse; and the odd polynomial O1 fits relatively poorly, but is substantially better than P1, P2, H1, A1, and A2.

In summary, the odd polynomial fitting is significantly better overall than the other types of fitting functions, and O3 fits best in the overall and linear intervals.

Characterization of odd polynomial fitting function

From Fig. 6a it can be concluded that the fitting effect of the polynomial fitting function increases with the increase in the order of the fit. As evident from Fig. 6d, the effect of fitting the odd polynomial fitting function increases as the order of the fit increases. Observing Table 2 shows that the polynomial fitting function R^2 increases with the order of the fit. Similarly, the odd polynomial fitting function R^2 increases with the order of the fit.

The R^2 and the number of coefficients of the fitted functions for polynomials of the same order P2, P4, P6, and odd polynomials O1, O2, and O3 in different intervals are compared, respectively. As can be seen from Table 2, only O1 has a significantly larger R^2 than P2 within different intervals, while the difference in R^2 between P4 and O2 and between P6 and O3 within different intervals is not significant. The number of coefficients of the polynomial fitting functions P2, P4, and P6 are 6, 8, and 10, respectively, while the number of coefficients of the odd polynomial O1, O2, and O3 are 4, 5, and 6, respectively. Therefore, compared to the polynomial fitting function of the same order, the odd

Polynomial has a smaller number of coefficients to be solved and a more straightforward functional form while at the same time not fitting poorly.

T a b l e 3. Fitting expressions and determination coefficient results for O3, P6, H3, and A3

Number	Fitting expression results	R^2
O3	$y = -0.01388 + 0.05407x - 2.056 \cdot 10^{-4}x^3 + 4.84 \cdot 10^{-7}x^5 - 5.369 \cdot 10^{-10}x^7 + 2.205 \cdot 10^{-13}x^9$	0.966
P6	$y = -0.0226 + 0.0491x + 0.0001196x^2 - 0.0001289x^3 - 2.556 \cdot 10^{-7}x^4 + 1.886 \cdot 10^{-7}x^5 + 2.139 \cdot 10^{-10}x^6 - 1.248 \cdot 10^{-10}x^7 - 6.043 \cdot 10^{-14}x^8 + 3 \cdot 10^{-14}x^9$	0.953
H3	$y = 0.4551 \tanh(0.1309x) - 0.02954 \tanh(156.4x)$	0.927
A3	$y = 0.5218 \arctan(0.1085x) - 0.007625x$	0.936

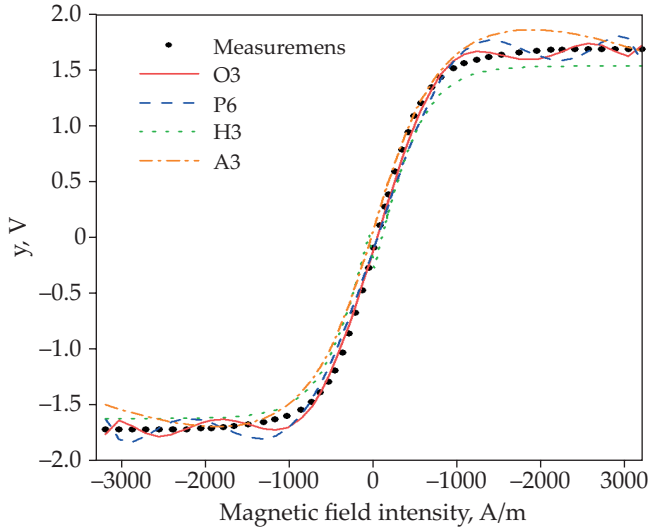

Fig. 7. Curve fitting results for O3, P6, H3, and A3, demonstrating the relationship between the applied magnetic field strength and the output voltage

In summary, similar to the polynomial, the odd polynomial can also improve the fitting effect by increasing the fitting order, and compared with the polynomial of the same order, the odd polynomial has less number of coefficients to solve and a simpler solution process under the premise of guaranteeing the fitting effect.

Fitting experiment of output characteristic curve of MR sensor

Experiments are designed to investigate the effectiveness of the basic magnetization curve fitting method based on spectral analysis applied to the output characteristic curve of an MR sensor.

TMR input/output data acquisition

The TMR input/output data measurement data can be obtained by changing the excitation signal amplitude and measuring the root-mean-square values of the excitation current i and the differential output voltage U simultaneously.

TMR output characteristic curve fitting

Odd polynomial fitting function O3, polynomial fitting function P6, hyperbolic tangent type fitting function H3, and arctangent type fitting function A3, which have the best fitting effect among the types of fitting functions in Table 2, are chosen as the fitting functions to fit the TMR input/output data measurement data based on the NLS method. The results of the fitted expressions and coefficients of determination for O3, P6, H3, and A3 are shown in Table 3, and results with R^2 values over 0.95 are shown in bold font, while results with the largest R^2 values are shown in italics. The curve fitting results for O3, P6, H3, and A3 are shown in Fig. 7.

Comparison of fitting results for odd polynomial fitting function

Fig. 7 shows that all four fitting functions O3, P6, H3, and A3 can reflect the trend of the TMR input/output measurement data as well as the nonlinear characteristics of the MR sensor, among which O3 and P6 have better fitting effects. Combined with Table 3, it is observed that the coefficients of determination for the four fitted functions O3, P6, H3, and A3 are 0.966, 0.953, 0.927, and 0.936, respectively, where odd polynomial fitting function O3 has the largest coefficient of determination, $R^2 = 0.966$, and the best fitting effect.

Table 3 shows that the number of coefficients to be solved for the four fitted functions O3, P6, H3, and A3 is 6, 10, 4, and 3, respectively, where hyperbolic tangent type fitting function H3 and arctangent type fitting function A3 have fewer coefficients to be solved but the mathematical operations of trigonometric functions are more complicated than exponential functions. Compared to the polynomial fitting function P6, the odd polynomial fitting function O3 is simpler in form and has fewer solution parameters.

In summary, the odd polynomial fitting function obtained based on spectral analysis is also suitable for fitting the output characteristic curve of MR sensors. The odd polynomial fitting function not only has a simple function expression but also has a better fitting effect.

CONCLUSIONS

In this paper, the output of the basic magnetization curve fitting results under sinusoidal excitation is analyzed spectrally. The odd polynomial fitting function is proposed based on significant odd harmonic amplitude characteristics. The application and effect of the odd polynomial on the basic magnetization curve and the fitting of the output characteristics of the MR sensor are investigated through comparative experiments. The odd polyno-

mial fitting function obtained based on spectral analysis can effectively fit the basic magnetization curve as well as the output characteristic curve of the MR sensor. Also, the odd polynomial fitting function has a better fitting effect on the basic magnetization curve, which can be further improved by increasing the fitting order. While compared to a polynomial fitting function of the same order, the odd polynomial fitting function has a smaller number of coefficients and simpler function expressions.

The reasonableness and effectiveness of applying the odd polynomial fitting function obtained based on spectral analysis to the basic magnetization curve fitting have been preliminarily verified. However, the application and effectiveness of the curve fitting results based on the odd polynomial need to be further investigated. Curve fitting with centrosymmetric features can also be considered to use odd polynomial fitting functions. The idea of constructing a fitting function from the results of spectral analysis provides a reasonable basis for the selection of the fitting function, and the idea can be generalized to other types of curve fitting.

Authors contribution

G.X. – writing-original draft, writing-review and editing, visualization, data curation; S.W. – methodology, formal analysis, writing-original draft, writing-review and editing, data curation; L.Z. – writing-original draft, writing-review and editing, supervision; L.W. – conceptualization, methodology, formal analysis, writing-original draft, writing-review and editing, supervision, data curation.

Funding

The Anhui Provincial Scientific Research Plan Program (2023AH051556) supported this work.

Conflict of interest

The authors declare no conflict of interest.

REFERENCES

[1] Silveyra J.M., Ferrara E., Huber D.L. *et al.*: *Science* **2018**, *362(6413)*, eaao0195. https://doi.org/10.1126/science.aao0195

[2] Calata J.N., Lu G.Q., Ngo K.: *Journal of Electronic Materials* **2014**, *43*, 126. https://doi.org/10.1007/s11664-013-2866-7

[3] Sunday K.J., Taheri M.L.: *Metal Powder Report* **2017**, *72(6)*, 425. https://doi.org/10.1016/j.mprp.2016.08.003

[4] Nyyssönen T., Hutchinson B., Broddefalk A.: *Materials Science and Technology* **2021**, *37(10)*, 883. https://doi.org/10.1080/02670836.2021.1963916

[5] Ripka P.: *Journal of Magnetism and Magnetic Materials* **2008**, *320(20)*, 2466. https://doi.org/10.1016/j.jmmm.2008.04.079

[6] Hui Y., Xing L., Shukang L. *et al.*: *Transactions of China Electrotechnical Society* **2023**, *38(19)*, 5128. https://doi.org/10.19595/j.cnki.1000-6753.tces.230965

[7] Pan C., Wang C.M., Cai G.W. *et al.*: *Electric Power Automation Equipment* **2014**, *34(4)*, 49. https://doi.org/10.3969/j.issn.1006-6047.2014.04.009

[8] Lin M.Y., Foe S.W., Mathew G. *et al.*: *IEEE Transactions on Magnetics* **2000**, *36(5)*, 2490. https://doi.org/10.1109/20.908483

[9] Boukhenoufa A., Dolabdjian C.P., Robbes D. *et al.*: *IEEE Sensors Journal* **2005**, *5(5)*, 916. https://doi.org/10.1109/JSEN.2004.841451

[10] Dalessandro L., Odendaal W.G.H., Kolar J.W.: *IEEE Transactions on Power Electronics* **2006**, *21(5)*, 1167. https://doi.org/10.1109/TPEL.2006.880357

[11] Ponjavic M.M., Duric R.M.: *IEEE Sensors Journal* **2007**, *7(11)*, 1546. https://doi.org/10.1109/JSEN.2007.908234

[12] Ando B., Baglio S, La Malfa S. *et al.*: *IEEE Transactions on Instrumentation and Measurement* **2011**, *61(5)*, 1361. https://doi.org/10.1109/TIM.2011.2175827

[13] Davino D., Visone C., Ambrosino C. *et al.*: *Sensors and Actuators A: Physical* **2008**, *147(1)*, 127. https://doi.org/10.1016/j.sna.2008.04.012

[14] Wang J., Liu M.G.: *Electric Machines and Control Application* **2017**, *44(7)*, 26.

[15] Lee H.C., Chen C.W., Wei S.W.: *IEEE Transactions on Communications* **2010**, *58(3)*, 733. https://doi.org/10.1109/TCOMM.2010.03.080053

[16] Murariu G., Condurache-Bota S., Tigau N.: *International Journal of Modern Physics B* **2012**, *26(7)*, 3155. https://doi.org/10.1142/S021797921250049X

[17] Xu X., Cisewski-Kehe J., Davis A.B. *et al.*: *The Astronomical Journal* **2019**, *157(6)*, 243. http://doi.org/10.3847/1538-3881/ab1b47

[18] Mecozzi M.: *APCBBE Procedia* **2014**, *10*, 2. https://doi.org/10.1016/j.apcbee.2014.10.003

[19] Zhou B., Ye H.: *Journal of Process Control* **2016**, *37*, 21. https://doi.org/10.1016/j.jprocont.2015.11.003

[20] Fu T., Yang K., Li S.: *Forum of South China* **2018**, *49(23)*, 50.

[21] Sandeep V., Murthy S.S., Singh B.A.: "A comparative study on approaches to curve fitting of magnetization characteristics for induction generators", Materials from IEEE International Conference on Power Electronics, Drives and Energy Systems, Bengaluru, India, December 16-19, 2012.

https://doi.org/10.1109/PEDES.2012.6484362
[22] Zhao D.D., Liu S., Cao D.P.: *Journal of Magnetic Materials and Devices* **2012**, *43(6)*, 24.
[23] Jing P., Tian M., Zhang H.: "Winding Design and Control Method of a Novel Quick Response Magnetic-valve Controllable Reactor", Materials from 22nd International Conference on Electrical Machines and Systems, Harbin, China, August 11-14, 2019.
https://doi.org/10.1109/ICEMS.2019.8922032
[24] Tang Q., Wang Z., Anderson P.I. *et al*.: *IEEE Transactions on Magnetics* **2015**, *51(5)*, 8400708.
https://doi.org/10.1109/TMAG.2014.2372672
[25] Silveyra J.M., Conde Garrido J.M.: *Journal of Magnetism and Magnetic Materials* **2021**, *540*, 168430.
https://doi.org/10.1016/j.jmmm.2021.168430
[26] Silveyra J.M., Conde Garrido J.M.: *JOM* **2023**, *75*, 1810.
https://doi.org/10.1007/s11837-023-05704-x
[27] Silveyra J.M., González M.I, González T.F. *et al*.: *IEEE Transactions on Magnetics* **2024**, *60(9)*, 7001406.
https://doi.org/10.1109/TMAG.2024.3408681
[28] Éfendiyev É H., Ali-zade R.A., Zubov V.P.: *Crystallography Reports* **2005**, *50*, S168.
https://doi.org/10.1134/1.2133995
[29] Filipcsei G., Csetneki I., Szilágyi A. et al.: "Magnetic Field-Responsive Smart Polymer Composites" in "Oligomers – Polymer Composites – Molecular Imprinting" (edit. Gong B., Sanford A.R., Ferguson J.S.), Springer Berlin, Heidelberg 2007, p. 137.
https://doi.org/10.1007/12_2006_104
[30] Prasanna G.D., Jayanna H.S., Lamani A.R. *et al*.: *Synthetic Metals* **2021**, *161(21-22)*, 2306.
https://doi.org/10.1016/j.synthmet.2011.08.039
[31] Xue S., Yang Y.: *The Journal of Navigation* **2017**, *70(4)*, 810.
https://doi.org/10.1017/S0373463317000030
[32] Zhu Y.H., Yu Z.S., Xiang X.L.: *Metal Functional Materials* **2016**, *23(5)*, 41.
[33] Renaud O., Victoria-Feser M.P.: *Journal of Statistical Planning and Inference* **2010**, *140(7)*, 1852.
https://doi.org/10.1016/j.jspi.2010.01.008
[34] Lipsitz S.R., Leong T., Ibrahim J. *et al*.: *Journal of the Royal Statistical Society Series D (The Statistician)* **2010**, *50(1)*, 87.
https://doi.org/10.1111/1467-9884.00263
[35] Talebian S., Hojjat Y., Ghodsi M. *et al*.: *Journal of Magnetism and Magnetic Materials* **2015**, *396*, 38.
https://doi.org/10.1016/j.jmmm.2015.08.006
[36] Murthy S.S., Singh B., Sandeep V.: *IET Electric Power Applications* **2013**, *7(6)*, 477.
https://doi.org/10.1049/iet-epa.2011.0360

Received 9 XII 2024.
Accepted 9 I 2025.